ORIGINAL ARTICLE

Deep learning model for predicting tunnel damages and track serviceability under seismic environment

Abdullah Ansari[1] · K. S. Rao[1] · A. K. Jain[1] · Anas Ansari[2,3]

Abstract

Jammu and Kashmir in the northwestern part of the Himalayan region is frequently triggered with moderate to large magnitude earthquakes due to an active tectonic regime. In this study, a mathematical formulation-based Seismic Tunnel Damage Prediction (STDP) model is proposed using the deep learning (DL) approach. The pertinency of the DL model is validated using tunnel damage data from historical earthquakes such as the 1999 Chi-Chi earthquake, the 2004 Mid-Niigata earthquake, and the 2008 Wenchuan earthquake. Peak ground acceleration (PGA), source to site distance (SSD), overburden depth (OD), lining thickness (t), tunnel diameter (Φ), and geological strength index (GSI) were employed as inputs to train the Feedforward Neural Network (FNN) for damage state prediction. The performance evaluation results provided a clear indication for further use in a variety of risk assessment domains. When compared to models based on historical data, the proposed STDP model produces consistent results, demonstrating the robustness of the methodology used in this work. All models perform well during validation based on fitness metrics. The "STD multiple graphs" is also proposed which provide information on damage indexing, damage pattern, and crack predictive specifications. This can be used as a ready toolbox to check the vulnerability in post-seismic scenarios. The seismic design guidelines for tunnelling projects are also proposed, which discuss the damage pattern and suggest mitigation measures. The proposed STDP model, STD multiple graphs, and seismic design guidance are applicable to any earthquake-prone tunnelling project anywhere in the world.

Keywords Deep learning · Seismic damage · Tunnelling · Neural network · Prediction model · Track serviceability

Introduction

Seismic damages to infrastructure projects are unavoidable due to natural, environmental, and field-specific operational influence factors. Due to the gradual nature of the damage, it is vital to evaluate infrastructures regularly to avoid any structural perversion. Unfortunately, tunnels and associated infrastructure damages due to the 1995 Kobe earthquake and 2016 Kumamoto earthquake in Japan, the 1999 Chi-Chi earthquake in Taiwan, and the 2008 Wenchuan earthquake in China discarded the belief in the structural safety of underground structures during seismic events (Zhang et al. 2018; Tsindis et al. 2020; Wang et al. 2021).

Jammu and Kashmir is located in the northwestern Himalayas, which is one of the world's most active seismic regions, with major earthquakes provoked in 1555, 1828, 1885, 1905, and 2005. The 2005 Kashmir earthquake (M_w=7.6) was one of the worst, with over one lakh people killed and infrastructure projects including bridges, retaining walls, and dams destroyed (Durrani et al. 2005). This area has witnessed mega infrastructural projects including bridge abutment, tunnelling, and expansion of railway tracks and national highways, which are going to help the overall economic development of the region (Ansari et al. 2022a, b). The Udhampur Srinagar Baramulla Rail Link (USBRL) project is a 345 km long mega rail project in the Himalayan terrain that is bordered by active seismic sources such as the Main Boundary Thrust (MBT) and Main Central Thrust (MCT). The major tectonic source and alignment of the USBRL project are shown in Fig. 1. The construction work of major tunnel projects started after the 2005 Kashmir

✉ Abdullah Ansari
  aamomin183@gmail.com

[1] Department of Civil Engineering, Indian Institute of Technology Delhi, Hauz Khas, New Delhi 110016, India

[2] Department of Computer Engineering, Sanjivani College of Engineering, Kopargaon, Maharashtra 423603, India

[3] School of Electronic and Computer Science, University of Southampton, Southampton SO17, England, UK

earthquake. The growing infrastructural projects, together with the previous historical record of earthquakes and seismotectonic settings push to examine the seismic damage of tunnels for post-seismic phases.

Mathematical modelling is the process of describing a real-world problem in mathematical terms, usually in the form of equations, and then using these equations to both understand the original problem and discover new features about it (Foucquier et al. 2013; Xia et al. 2022). The mathematical models can be used to analyze structural behaviour in response to earthquakes (Harichandran and Vanmarcke 1986; Özdamar and Pedamallu 2011; Valaskova et al. 2018). Problem-driven mathematical models of natural and social phenomena in which the selection of relevant mathematics is part of the problem-solving process (Zhang et al. 2022). To solve the earthquake shelter location-allocation problem, a multi-objective, hierarchical mathematical model was developed, along with an interleaved modified particle swarm optimization algorithm and genetic algorithm (Ihueze and Onwurah 2018; Zhao et al. 2019). Modelling underpins much of our understanding of the world and enables tunnel engineers to design earthquake-resistant

underground structures. In the current study, six variables from the data set of the Himalayan region are used as input layers, including peak ground acceleration (PGA), source to site distance (SSD), overburden depth (OD), lining thickness (t), tunnel diameter (Φ), and geological strength index (GSI), and a Feedforward Neural Network (FNN) is trained using a deep learning approach. The training and adaptation learning functions were represented by TRAINLM and LEARNGDM, respectively. The cumulative weightage factor for the output layer was provided by FNN. After the neurons have been trained, target data are used to verify the network's robustness. Through conceivable hits and trials, the weightage elements are resolved, and a mathematical equation in terms of damage index is developed. The Seismic Tunnel Damage Prediction (STDP) Model proposed in the present study is compared with the tunnel damage data sets from the 1999 Chi-Chi earthquake, the 2004 Mid-Niigata earthquake, and the 2008 Wenchuan earthquake.

For the 2004 Mid-Niigata earthquake, the R-value for the suggested STDP model and the NETD model is nearly comparable. The MAE for the CETD Model differs from others since the data set for the Chi-Chi earthquake was found
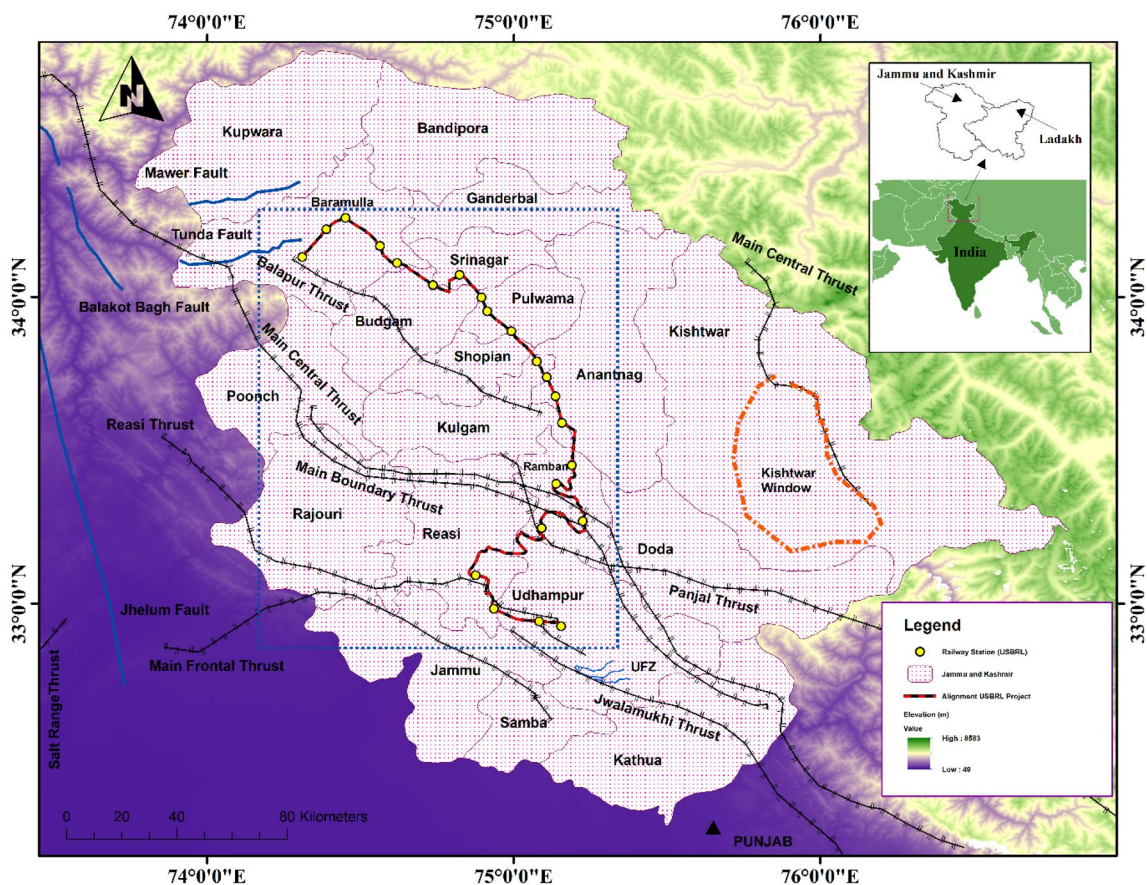

Fig. 1 Map of Jammu and Kashmir in NW Himalayas showing active seismic sources and alignment of Udhampur Srinagar Baramulla Rail Link (USBRL) project

to be unevenly distributed. When compared to the WETD model, the DL neural network computes a larger value of R. The "STD multiple graphs" is presented which have a four-sector graph based on the logical order of the input variables. Seismic design guidelines for tunnelling projects are also proposed in earthquake-prone areas. This diagram provides information on damage indexing, damage pattern, and crack predictive specification. It also analyzes the risks involved and the implications for transportation network serviceability. Mitigation measures must also be implemented for all expected damage states. The proposed seismic tunnel damage prediction (STDP) model, STD multiple graphs, and design guidance can be applied to any earthquake-prone tunnelling project worldwide.

Seismic tunnel damages

The roadway and railway are the two most convenient modes of transportation. The availability of space is a major mishap for the establishment of such networks. To overcome this, underground spacing is an outstanding alternative and this leads to an increase in the demand for tunnel construction. The earthquake-resistant design of such infrastructure projects is extremely challenging. The 1995 Kobe earthquake in Japan caused major damage to tunnels and underground infrastructure, disrupting the entire transportation network (Hashash et al. 2001). One of the devastating incidents in 1999 was the Chi-Chi earthquake in Taiwan, which damaged 49 of the 57 tunnels. The tunnel portals have been severely damaged, with minor to moderate level cracking as well as spalling in the tunnel lining (Wang et al. 2021). During 2004 Mid Niigata earthquake in Japan injured over 4790 people,

demolished or collapsed more than 0.1 million dwellings, and damaged 49 tunnels (Jiang et al. 2010).

The 2005 Kashmir earthquake triggered the whole state of Jammu and Kashmir resulting in infrastructure and socio-economic loss (Ansari et al. 2022a). During this event, the unlined northern portal of the Muzaffarabad tunnel collapsed (Durrani et al. 2005; Aydan et al. 2010). Following the 2005 Kashmir earthquake, the 2008 Wenchuan earthquake in China (M_w=8) destroyed billions of dollars in property and infrastructure losses, particularly in hilly tunnels along the Wenchuan highway (Roy and Sarkar 2017). This earthquake was one of the most tremendous earthquakes in the Asian continent affecting around 0.2 million people in China. This earthquake primarily damaged the 52 highway tunnels in mountainous areas (Lai et al. 2017).

Shrestha et al. (2020) highlighted the damages to the Melamchi tunnel in Nepal, which were caused by the 2015 Gorkha earthquake (Fig. 2). The 2016 Kumamoto earthquake is the most recent example of a large magnitude (M_w=7.3) earthquake inflicting damage to underground infrastructure, notably the Tawarayama tunnel, which is located 22.4 km from the main event's epicenter (Zhang et al. 2018). In Europe, similar to the damage to the Bolu tunnel in Turkey in 1999, the San Bendetto tunnel in Italy was destroyed by the Norcia earthquake in 2016 (Callisto and Ricci 2019). Table 1 shows the specifics of tunnels that have been damaged by significant earthquakes.

Lining spalling and portal collapses were the most visible seismic damage in multiple mountain tunnels during the 1999 Chi-Chi earthquake and the 2008 Wenchuan earthquake During these two earthquakes, most of the tunnels exhibit extensive lining deformation. The two principal portal failure types are stratum deformation and spandrel cracking (Ansari et al. 2022a, b). The most typical types

Table 1 List of tunnels damaged during major earthquake events

| Tunnel name	Location	Magnitude (M_w)	Event date	References
San Bendetto	Norcia (Italy)	6.2	Oct 26, 2016	Callisto and Ricci (2019)
Tawarayama	Kumamoto (Japan)	7.3	April 16, 2016	Zhang et al. (2018)
Melamchi	Melamchi, Bagmati (Nepal)	7.8	April 25, 2015	Shrestha et al. (2020)
Longxi	Wenchuan (China)	8.0	May 12, 2008	Wang and Zhang (2013)
Muzaffarabad	Muzaffarabad (Pakistan)	7.6	October 8, 2005	Durrani et al. (2005)
Uonuma	Niigata (Japan)	6.8	October 23, 2004	Jiang et al. (2010)
Intake tunnel of Omiya Dam	Western Tottori (Japan)	7.3	October 8, 2000	Dalguer et al. (2003)
Tottori	Western Tottori (Japan)	7.3	October 8, 2000	Dalguer et al. (2003)
Intake tunnel of Shih-Gang Dam	Chi-Chi (Taiwan)	7.6	September 23, 1999	Ohmachi (2000)
Bolu	Izmit (Turkey)	7.4	August 17, 1999	Kontoe et al. (2008)
Outlet tunnel of Kakkonda 2 hydropower station	Mid-north Iwate (Japan)	6.1	September 3, 1998	Konagai et al. (2005)
Rokko	Kobe (Japan)	7.2	January 1, 1995	Asakura and Sato (1996)
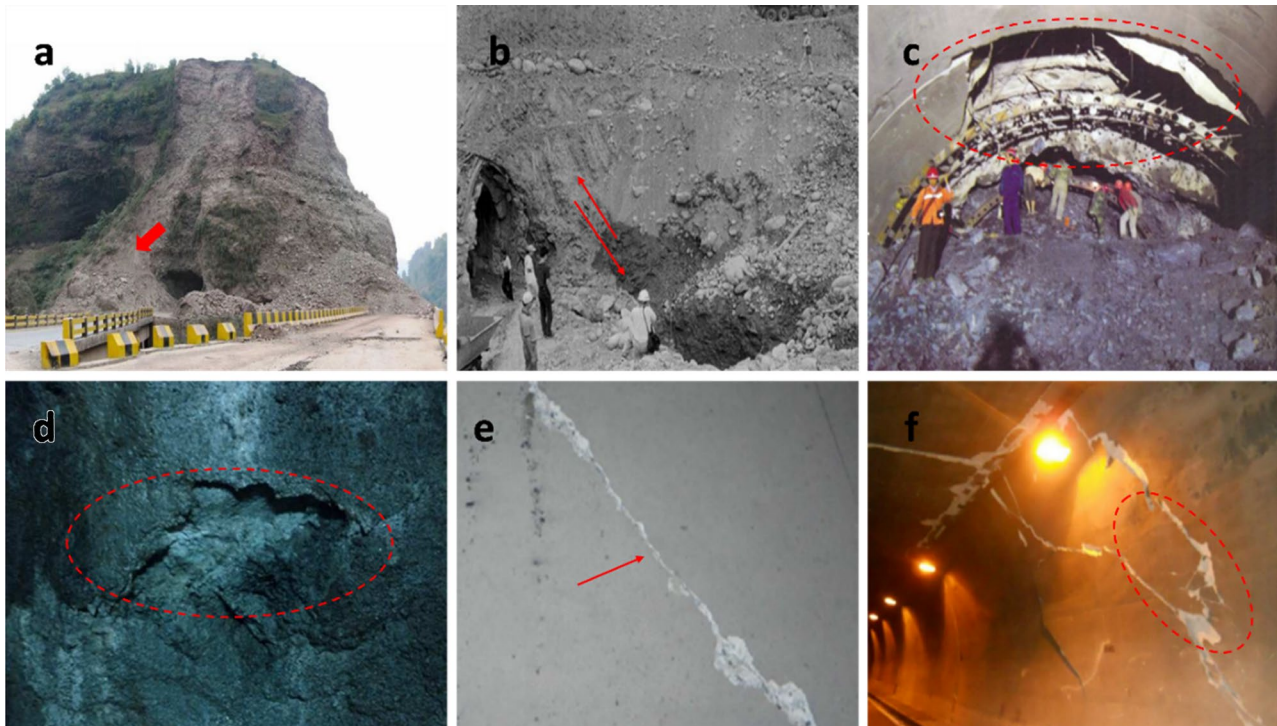
Fig. 2 Illustration of seismic tunnel damages **a** collapse of the unlined portal during 2005 Muzaffarabad earthquake (Durrani et al. 2005); **b** sheared-off liner during 1999 Chi-Chi earthquake (Wang et al. 2021); **c** lining collapse during 2008 Wenchuan earthquake (Yu et al. 2016); **d** spalling and shotcrete falling during 2015 Gorkha earthquake (Shrestha et al. 2020); **e** inclined cracks during 2016 Kumamoto earthquake (Zhang et al. 2018) and **f** transverse ring cracks during 2016 Norcia earthquake (Callisto and Ricci 2019)

of pavement damage seen in tunnels affected by large magnitude earthquakes are uplift, cracking, and groundwater leakage in construction joints and concrete lining (Yu et al. 2016). The majority of the tunnels damaged in the 2004 Niigata earthquake had wall deformation, with heaving mechanisms at the bottom slab and distorted sidewalls (Wang et al. 2021). A few typical examples of seismic tunnel damage are presented in Fig. 2.

Deep learning and its applications for earthquake problems

Conceptualization of deep learning and neural networking

Soft computing assists users in solving real-world problems by giving approximate solutions that traditional and analytical models cannot offer. Artificial intelligence (AI) has grown in popularity and acceptance among researchers in fields such as engineering, technology, medicine, cognitive science, mathematics, and so on. AI is like biology or mathematical science that examines how to construct intelligent systems that can solve problems creatively by replicating human capabilities (Hinton and Salakhutdinov 2012; Zhang

et al. 2021). In terms of machine learning (ML), it is a subset of AI that allows systems to automatically learn and improve from experience without being explicitly designed (Jordan and Mitchell 2015). Deep neural learning, or DL, is a type of ML that gains enormous strength and flexibility by learning to represent the world as a layered hierarchy of concepts without explicitly extracting characteristics (Fig. 3). Under the assumption of no noise, the accuracy of DL predictions will gradually improve as the dataset grows (Talkhablou et al. 2019; Meraj et al. 2021). It essentially gives effective tools for dealing with the data and extracting useful information for accurate decision-making. Feedforward, recurrent, convolutional, and generative adversarial are the four DL models useful for various engineering applications.

Artificial Neural Network (ANN) adheres to the biological learning process that exists in the human brain, intending to create a highly intelligent system that corresponds to neurons (Fukushima and Miyake 1982; Barrow 1996). Feedforward Neural Network (FNN) consists of three layering systems including input, output, and hidden (Phoon 2020). This is mostly used to solve complex judicial-specific modelling and mathematical formulations. A recurrent Neural Network (RNN) has the unique ability to detect past data based on real-time judgmental ideas (Pascanu et al. 2013). LSTM is a more advanced variant
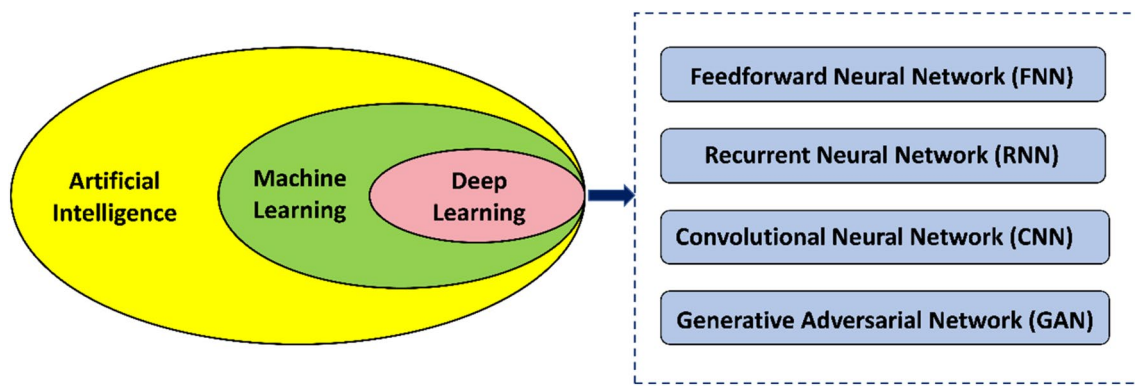
Fig. 3 Conceptual relationship between the existing soft computing techniques

of RNN that has three gate controllers known as the input, forget, and output gates (Yuan et al. 2019; Chen et al. 2020). Every piece of information that passes through this unit must be chosen whether it should be remembered or forgotten, and then assigned to the appropriate gate. For image identifications, pictorial representation, and decorative modelling, Convolutional Neural Network (CNN) is popular which works based on the stability of kernels. In the field of infrastructure and transportation engineering, the CNN model is applicable for traffic signal design. For the case of Generative Adversarial Network (GAN), parallel training of generator and discriminator is performed for fake samples.

Applications of deep learning algorithms

The earthquake-related problems are bristling with uncertainty and involve numerous elements that cannot be directly determined by seismologists and geophysicists. The researchers use soft computing technologies to handle numerous seismic effects-based challenges and assessment issues. DL technique is useful to handle big data with perfection and defined grouping for engineering problems. AI can handle randomized searches and approximate reasoning. Transfer learning techniques can be used for prediction modelling by employing ML algorithms (Abdulnaby et al. 2016; Alhassan et al. 2018; Biswas et al. 2018). Unsupervised clustering methods are required for damage prediction in ML-based transportation network assessment projects. Table 2 enlists the various applications of deep learning

Table 2 Practicable applications of soft computing in the earthquake domain

DL neural network	Applications	References
CNN	Teleseismic detection for ground motion	Dickey et al. (2019)
CNN	Seismic phase detection	Zhu et al. (2019)
RNN	Pavement crack detection	Zhang et al. (2018)
CNN	Shield tunnel lining defects	Xue and Li (2018)
CNN	Earthquake-induced reinforced concrete columns damage	Xu et al. (2019)
CNN	Building damage vulnerability in post-seismic scenarios	Nahata et al. (2019)
RNN + CNN	Structural damage detection	Dang et al. (2021)
FNN + GAN	Geophysical exploration for subsurface investigations	Dimililer et al. (2021)
CNN + RNN	Signal processing for detection of seismic waves	Kong et al. (2019)
FNN	Post-seismic evaluation of building damages	Zhang and Pan (2022)
ANN	Seismic design of deep tunnels	Ornthammarath et al. (2008)
FNN	Seismic damage to buildings	Patterson et al. (2018)
ANN	Fragility functions for underground structures in soft soils	Huang et al. (2022)
FNN	Ground motion parameters prediction modelling	Derakhshani and Foruzan (2019)
LSTM	Post-seismic building damage classification	Mangalathu and Burton (2019)
FNN + CNN	Damage scenario-based seismic response	Kim et al. (2020)
CNN	Prediction of earthquake magnitude	Huang et al. (2018)

algorithms in the field of earthquake engineering, disaster risk, geophysical modelling, and mathematical predictions.

Architecture of algorithm for the proposed prediction model

Selection of input variables

Tunnelling involves various difficult situations such as squeezing, creeping, water infiltration, shear zone creation, faulting, and so on. Aside from this, a few uncertain circumstances, such as impact and blast loading, may occur. In such instances, predictive modelling comes into play and provides an estimate of the future damage states. For important problems like intersecting tunnels, anisotropic conditions, and geological variability overlain by seismic, impact, or blast loading, mathematical formulation-based predictive modelling serves as a ready-to-use toolbox. The practical application of DL is expanding, particularly in the realm of mathematical modelling (Kochhar et al. 2022; Biswas and Sinha 2021; Nanda et al. 2021; Raaj et al. 2022). In this study, an algorithm based on the Feedforward Neural Network (FNN) is utilized to create a prediction model of future damages caused by seismic loading. Peak ground acceleration (PGA), source to site distance (SSD), overburden depth (OD), lining thickness (t), tunnel diameter (Φ), and geological strength index (GSI) are passed down to create the input layers of the neural network. These input parameters were taken from the previously conducted site-specific seismic studies for the Jammu and Kashmir (Ansari et al. 2022a) as well as technical reports of the Udhampur Srinagar Baramulla Rail Link (USBRL) project (Rajesh 2013; Ram 2015;

Yusoff and Adhikari 2017; Sharma and Manchanda 2018; Singh and Sherpuri 2018; Riella et al. 2019). The Udhampur Srinagar Baramulla Rail Link (USBRL) project, a 345 km long railway line connecting the Baramulla with the Indian Railways network offers Jammu and Kashmir an easy way of transportation option (Tomar 2013; Sharma and Panwar 2017; Wani and Alamgir 2017; Kumar 2018; Rohilla and Surinder 2018; Ahmad and Dhang 2019; Wingler 2020). The sectional length of Udhampur-Katra, Katra- Quazigund, and Quazigund -Baramulla are commissioned for traffic and works are in various stages of progress with mean sea level (MSL) varying from 660 to 1723 m. The alignment and structural details for each subsection are mentioned in Table 3.

Table 4 provides the details for the input parameters used in the present study. For each layer, five distinct classes are suggested. All these classes and their frequency distribution are presented in Fig. 4.

Model formulation

In this work, 70% of the training input–output datasets were used to train FNN, while 30% of the testing datasets were used to validate the competence of FNN using MATLAB chronic trait. The correlation between input layers and output layers was generated in FNN by establishing a chain of interconnected neurons (Fig. 5). The input and output variables are defined by x = (PGA, SSD, OD, t, Φ, GSI) and y = (Damage Index), respectively. When using the training dataset to analyze the intricate yet orderly network, the neurons are joined into numerous layers and weight is assigned to each neuron repeatedly. Following a series of trial and error simulations, it was contrived that a normal three hidden

Table 3 Comprehensive detailing of the subsections of the USBRL project

Parameters	Subsections			
	Udhampur-to-Katra (UD-KT)	Katra-to-Banihal (KT-BN)	Banihal-to-Quazigund (BN-QZ)	Quazigund-to-Baramulla (QZ-BR)
Completion Cost (In Crores)	1111	21,821	1992	3430
Cost per km (In Crores)	44	194	94	30
Total Stations	3	10	1	15
Route length (km)	25	111	18	118
Maximum Curvature	5º	4.86º	3.1º	2.75º
Tunnels				
Total Tunnels	10	27	1	0
Length (km)	11	164	11.21	0
Percentage Length in Tunnel (%)	44	87	62	
Bridges				
Total Bridges	50	37	35	809
Length (km)	1.48	7.035	0.28	4.21

Table 4 Parametric contributions of inputs employed for modelling

Tunnel	Micro-zonation zone	Fault/Thrust	Peak ground acceleration (PGA) g	Source to site distance (SSD) km	Overburden depth (OD) km	Lining thickness (t) mm	Tunnel diameter (Φ) m	Geological strength index (GSI)	Land-slide prone
T46P1.3	A	PT	0.343	8.2	367	600	8	39	Y
T46P2.2	A	MBT	0.711	6.3	256	300	5	35	Y
T44/45P1.2	A	MBT	0.711	4.8	575	300	7	33	Y
T46P2.3	A	PT	0.343	8.3	367	300	8	40	Y
T5P2.3	A	RT	0.831	6.4	359	300	7	36	Y
T44/45P2.2	A	MBT	0.711	5.3	877	300	5	34	Y
T5P1.3	A	RT	0.831	6.8	387	300	6	37	Y
T46P1.2	A	MBT	0.711	7.4	456	600	7	38	Y
T42/43P1.2	A	MBT	0.711	10.1	256	450	8	41	Y
T42/43P1.1	A	MCT	0.821	10.3	245	450	6	42	Y
T40/41P1.2	A	MBT	0.711	11.5	245	600	7	45	Y
T42/43P2.1	A	MCT	0.821	10.7	357	600	5	43	Y
T74RP1.1	A	MCT	0.821	11.9	130	600	6	48	Y
T42/43P2.2	A	MBT	0.711	11.3	578	600	6	44	Y
T44/45P1.1	A	MCT	0.821	11.8	377	600	7	47	Y
T74RP2.1	A	MCT	0.821	12.5	130	600	8	53	Y
T46P1.1	A	MCT	0.821	12.1	256	600	5	51	Y
T23P1.2	A	JT	0.69	16.9	119	600	7	34	N
T40/41P1.1	A	MCT	0.831	12.1	422	600	8	49	Y
T44/45P2.1	A	MCT	0.821	12.1	459	600	5	50	Y
T40/41P2.1	A	MCT	0.821	12.4	367	600	6	52	Y
T40/41P2.2	A	MBT	0.711	11.8	788	750	6	46	Y
T46P2.1	A	MCT	0.821	12.8	457	750	7	54	Y
T15P1.1	A	MCT	0.821	17.1	398	600	5	35	N
T14P1.2	A	MBT	0.711	17.8	456	600	8	37	N
T15P2.1	A	MCT	0.821	16.8	656	600	8	33	N
T14P2.4	A	RT	0.831	17.8	376	600	7	38	N
T14P1.1	A	MCT	0.821	18.5	343	600	8	40	N
T74RP1.2	A	MBT	0.711	17.8	654	300	6	39	Y
T74RP2.2	A	MBT	0.711	18.8	654	300	5	41	Y
T14P2.1	A	MCT	0.821	17.5	877	600	7	36	N
T14P1.3	A	PT	0.343	23.4	354	600	5	48	N
T13P1.2	A	MBT	0.711	22.9	235	600	6	43	Y
T13P2.1	A	MCT	0.821	22.7	150	600	7	42	Y
T13P2.3	A	PT	0.343	26.2	298	600	8	42	Y
T25P2.1	A	RT	0.831	24.3	196	600	6	33	N
T5P2.2	A	JT	0.69	24.9	277	600	7	35	Y
T25P1.2	A	JT	0.69	25.4	196	600	5	37	N
T5P1.2	A	JT	0.69	24.7	381	600	6	34	Y
T10P2.2	A	MBT	0.711	25.4	242	600	8	36	N
T12P2.2	A	MBT	0.711	23.1	467	600	5	44	N
T11P1.2	A	MBT	0.711	23.2	543	600	7	45	N
T10P1.3	A	PT	0.343	28.7	325	600	8	37	N
T23P1.1	A	RT	0.831	23.7	230	600	5	50	N
T23P2.2	A	JT	0.69	26.4	119	500	6	43	N
T15P1.2	A	MBT	0.711	23.2	572	500	7	47	N
T11P2.2	A	MBT	0.711	23.6	462	500	8	49	N

Table 4 (continued)

Tunnel	Micro-zonation zone	Fault/Thrust	Peak ground acceleration (PGA) g	Source to site distance (SSD) km	Overburden depth (OD) km	Lining thickness (t) mm	Tunnel diameter (Φ) m	Geological strength index (GSI)	Land-slide prone
T6P2.3	A	PT	0.343	28.2	478	500	5	36	N
T6P1.3	A	PT	0.343	26.8	785	500	6	33	N
T14P2.3	A	PT	0.343	28.8	327	500	7	39	N
T23P2.1	A	RT	0.831	25.5	230	500	8	38	N
T13P1.4	A	RT	0.831	25.7	235	500	6	39	Y
T25P1.1	A	RT	0.831	23.8	385	600	8	51	N
T11P2.3	A	PT	0.343	30.5	367	600	5	33	N
T13P2.4	A	RT	0.831	25.8	322	600	6	41	Y
T10P2.3	A	PT	0.343	29.1	455	600	7	41	N
T5P2.1	A	MBT	0.711	27.8	295	600	8	35	Y
T12P1.2	A	MBT	0.711	23.2	873	600	5	46	N
T6P1.2	A	MBT	0.711	26.5	355	600	6	44	N
T15P2.2	A	MBT	0.69	24.1	632	600	7	52	N
T5P1.1	A	MBT	0.711	27.7	378	350	8	34	Y
T6P2.2	A	MBT	0.711	26.7	378	350	5	45	N
T10P1.2	A	MBT	0.711	25.8	644	350	6	40	N
T12P1.3	A	PT	0.343	31.1	356	350	7	36	N
T14P2.2	A	MBT	0.711	24.2	687	350	5	53	N
T25P2.2	A	JT	0.69	28.8	231	350	6	40	N
T13P1.3	A	PT	0.343	32.1	150	350	7	42	Y
T11P1.3	A	PT	0.343	30.1	435	350	8	45	N
T13P1.1	A	MCT	0.821	29.4	150	350	6	42	Y
T12P2.3	A	PT	0.343	31.7	577	350	8	40	N
T12P2.1	A	MCT	0.821	29.7	367	350	7	43	N
T14P1.4	A	RT	0.831	28.7	673	600	8	38	N
T11P2.1	A	MCT	0.821	30.7	467	600	5	34	N
T13P2.2	A	MBT	0.711	32.2	235	600	6	43	Y
T11P1.1	A	MCT	0.821	30.9	533	600	7	35	N
T6P1.1	A	MCT	0.821	31.2	566	600	5	37	N
T6P2.1	A	MCT	0.821	32.1	367	600	7	41	N
T12P1.1	A	MCT	0.821	29.8	746	600	8	44	N
T10P2.1	A	MCT	0.821	31.7	535	600	6	39	N
T10P1.1	A	MCT	0.821	31.3	743	600	7	38	N
T1P1.1	B	RT	0.831	4.6	104	600	5	33	N
T1P2.1	B	RT	0.831	4.2	176	600	6	45	N
T2P1.1	B	RT	0.831	4.1	235	600	7	44	N
T3P1.1	B	RT	0.831	6.2	105	300	6	35	N
T2P2.1	B	RT	0.831	5.2	366	300	5	34	N
T47P1.3	B	PT	0.343	9.2	363	300	6	41	Y
T3P2.1	B	RT	0.831	7.6	243	300	8	37	N
T47P1.2	B	MBT	0.711	7.3	567	600	8	36	Y
T47P2.3	B	PT	0.343	9.4	677	450	6	42	Y
T47P2.2	B	MBT	0.711	7.8	566	450	7	38	Y
T50P2.1	B	MCT	0.821	7.9	1032	600	7	39	Y
T50P1.1	B	MCT	0.821	8.9	864	600	5	40	Y
T47P1.1	B	MCT	0.821	13.2	357	600	6	43	Y
T50P2.3	B	PT	0.343	18.7	246	750	7	40	Y

Table 4 (continued)

Tunnel	Micro-zonation zone	Fault/Thrust	Peak ground acceleration (PGA) g	Source to site distance (SSD) km	Overburden depth (OD) km	Lining thickness (t) mm	Tunnel diameter (Φ) m	Geological strength index (GSI)	Land-slide prone
T50P1.2	B	MBT	0.711	15.4	368	750	5	45	Y
T50P1.3	B	PT	0.343	16.4	942	750	6	35	Y
T47P2.1	B	MCT	0.821	14.11	467	750	7	44	Y
T2P1.2	B	JT	0.69	18.7	265	600	6	39	N
T80P1.1	B	PT	0.343	17.1	1100	600	7	37	Y
T1P2.2	B	JT	0.69	19.4	123	600	5	42	N
T50P2.2	B	MBT	0.711	16.4	765	600	7	36	Y
T1P1.2	B	JT	0.69	19.6	98	600	8	43	N
T1P1.3	B	MFT	0.33	23.6	117	600	6	36	N
T2P2.2	B	JT	0.69	18.9	322	600	6	41	N
T80P2.1	B	PT	0.343	18.3	1100	600	7	38	Y
T1P2.3	B	MFT	0.33	23.8	165	300	5	39	N
T80P1.2	B	BT	0.741	15.4	1320	300	8	33	Y
T80P2.2	B	BT	0.741	15.8	1320	300	6	34	Y
T3P1.2	B	JT	0.69	23.2	210	600	8	33	N
T77DP1.1	B	MCT	0.821	21.3	454	600	5	44	Y
T2P2.3	B	MFT	0.33	27.8	189	600	8	42	N
T77DP2.1	B	MCT	0.821	23.3	454	600	7	34	Y
T77DP1.2	B	MBT	0.711	21.9	732	600	6	45	Y
T77DP2.2	B	MBT	0.711	23.7	732	500	5	37	Y
T3P2.3	B	MFT	0.33	29.6	245	500	7	43	N
T3P1.3	B	MFT	0.33	32.2	255	350	8	33	N
T2P1.3	B	MFT	0.33	32.2	255	350	5	45	N
T80P1.3	B	MCT	0.821	23.5	1320	350	7	35	Y
T80P2.3	B	MCT	0.821	23.7	1320	350	5	38	N
T3P2.2	B	JT	0.69	31.1	288	350	6	44	N
T80P2.4	B	MBT	0.711	27.2	1320	600	8	40	Y
T80P1.4	B	MBT	0.711	27.4	1320	600	6	41	Y
T2P2.5	B	MBT	0.711	32.9	587	600	5	34	N
T2P1.4	B	MCT	0.821	33.8	543	600	8	35	N
T2P2.4	B	MCT	0.821	34.2	654	600	6	36	N
T2P1.5	B	MBT	0.711	38.1	521	600	6	37	N
T49P2.1	C	MCT	0.821	7.5	335	450	5	39	Y
T48P2.2	C	MBT	0.711	8.8	672	450	5	40	Y
T49P1.1	C	MCT	0.821	7.3	1033	600	8	38	Y
T48P1.2	C	MBT	0.711	9.6	862	600	8	41	Y
T49P2.3	C	PT	0.343	14.1	932	750	8	45	Y
T49P1.3	C	PT	0.343	13.8	1008	750	5	44	Y
T49P2.2	C	MBT	0.711	13.3	789	750	8	42	Y
T78P1.1	C	MCT	0.821	14.3	758	750	8	40	Y
T48P1.3	C	PT	0.343	18.2	783	600	6	44	Y
T49P1.2	C	MBT	0.711	13.6	1105	600	5	43	Y
T78P2.1	C	MCT	0.821	15.2	758	600	7	41	Y
T78P1.2	C	MBT	0.711	16.7	639	600	5	42	Y
T48P2.3	C	PT	0.343	19.3	933	600	8	35	Y
T48P1.1	C	MCT	0.821	18.7	363	600	5	35	Y
T78P2.2	C	MBT	0.711	17.2	639	600	6	43	Y

Table 4 (continued)

Tunnel	Micro-zonation zone	Fault/Thrust	Peak ground acceleration (PGA) g	Source to site distance (SSD) km	Overburden depth (OD) km	Lining thickness (t) mm	Tunnel diameter (Φ) m	Geological strength index (GSI)	Land-slide prone
T48P2.1	C	MCT	0.821	18.6	356	300	7	45	Y
T46P1.3	A	PT	0.343	8.2	367	600	8	39	Y
T46P2.2	A	MBT	0.711	6.3	256	300	5	35	Y
T44/45P1.2	A	MBT	0.711	4.8	575	300	7	33	Y
T46P2.3	A	PT	0.343	8.3	367	300	8	40	Y
T5P2.3	A	RT	0.831	6.4	359	300	7	36	Y
T44/45P2.2	A	MBT	0.711	5.3	877	300	5	34	Y
T5P1.3	A	RT	0.831	6.8	387	300	6	37	Y
T46P1.2	A	MBT	0.711	7.4	456	600	7	38	Y

A Severe risk seismic zone, *B* High risk seismic zone, *C* Moderate risk seismic zone, *PT* Panjal Thrust, *RT* Reasi Thrust, *JT* Jhelum Thrust, *MBT* Main Boundary Thrust, *MCT* Main Central Thrust, *Y* Yes, *N* No
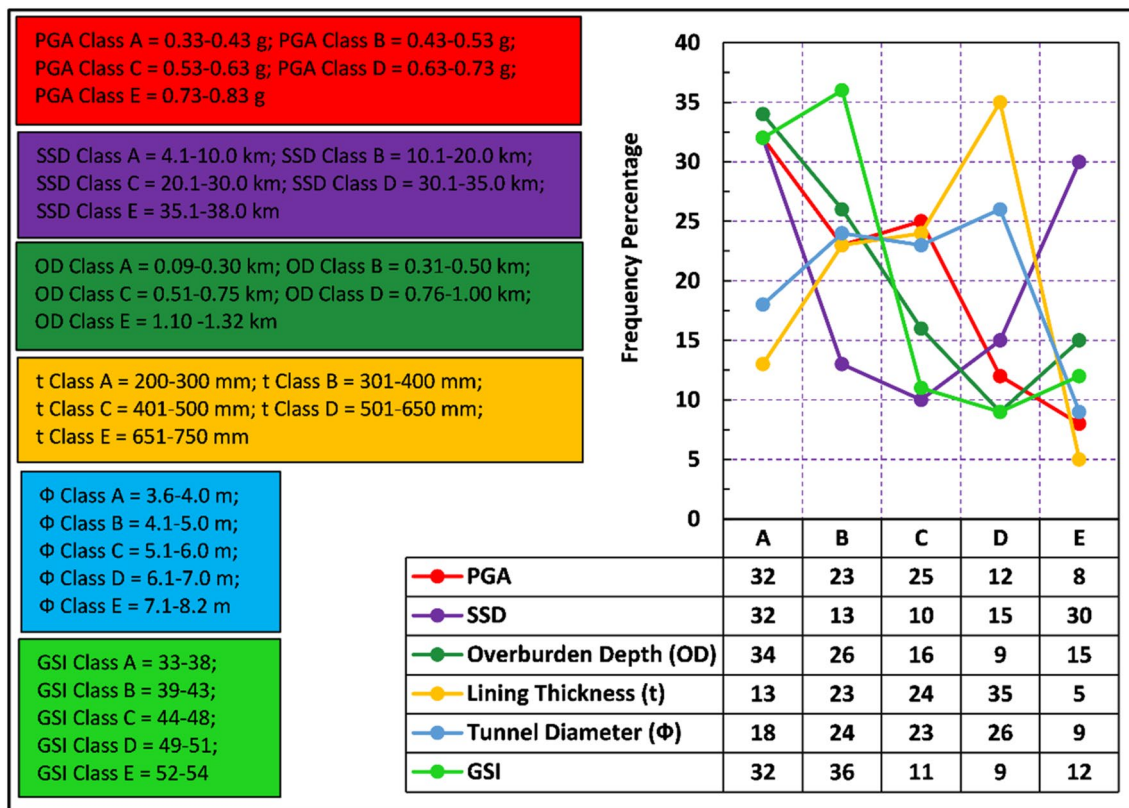
Fig. 4 Input parameters for operating the neural network

layers (H_1, H_2, H_3) of a neural network with 108 neurons yielded the best results. TRAINLM and LEARNGDM were used to represent the training and adaptation learning functions, respectively. LOG-SIG is a nonlinear activation function adopted for neurons in hidden layers. PURELIN is used as the transfer function for output layers. Table 5 provides the statistical context for the input parameters.

Methodology

The damage pattern of tunnels during previous earthquakes in Taiwan, Japan, and China show that underground structures are likewise vulnerable to extreme ground motion. Looking at previous devastation scenarios of tunnels and
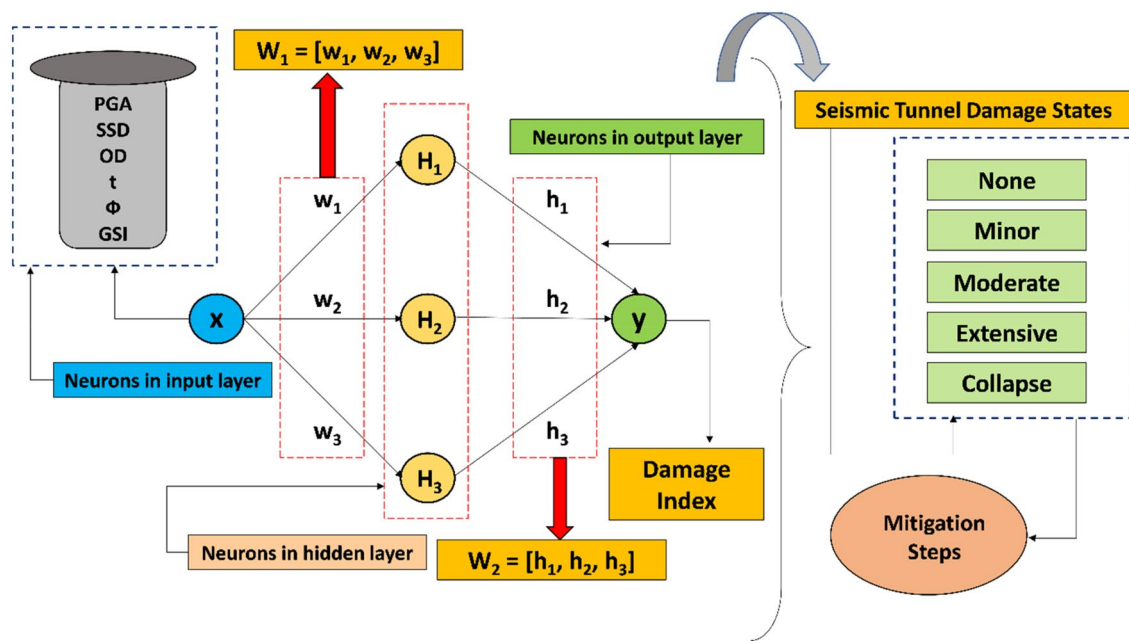
Fig. 5 Feedforward Neural Network (FNN) used in the present study

Table 5 Parametric contributions of inputs employed for STDP Model

Statistical variables	SSD (km)	Peak ground acceleration (PGA) g	Overburden depth (OD) km	Lining thickness (t) mm	Tunnel diameter (Φ) m	Geological strength index (GSI)
Mean	19.78	0.67	0.49	450	6.50	35
Median	19.32	0.71	0.38	375	6.30	30
Standard deviation	8.36	0.18	0.29	150	1.22	5.02
Range	34.00	0.50	1.23	550	4.60	21
Maximum	38.10	0.83	1.32	750	8.20	54
Minimum	4.10	0.33	0.09	200	3.60	33

accompanying transportation networks tightens the belt of safe seismic design for associated designers and tunnel experts. The tunnel damage states are authenticated based on the value ranges of the Damage Index (*DI*). *DI* is traditionally determined by dividing the actual bending moment (*M*) by the capacity bending moment (M_{RD}). From dynamic time history, the actual bending moment (*M*) is quantified based on the analytical approaches. The capacity bending moment (M_{RD}) is a material-dependent parameter, that can be estimated based on the material and geometrical properties of tunnels. In the present study, site-specific data are used to build a prediction model based on simplified factors. Special emphasis is placed on the ease of availability and significant contribution of variables from the input basket. Tunnel construction, installation, monitoring, and maintenance are difficult aspects of the infrastructure industry in the Jammu and Kashmir region. The frequency of earthquakes in the Himalayan region necessitates the development of a risk prediction technology capable of predicting damage patterns before the occurrence of actual seismic events.

Deep learning (DL) has advanced rapidly in recent years, with the potential to significantly alter and enhance the role of data science in a wide range of problems dealing the infrastructure resilience. Hoang and Tran (2019) demonstrated the validity of using metaheuristics to solve optimization problems in project and construction management, where metaheuristics are high-level procedures that find, generate or select heuristics for optimization. DL algorithms have been implemented in a variety of site safety problems subjected to disaster orientation (Kalakonas and Silva 2022; Mosavi et al. 2018; Falcone et al. 2020; Bernardi et al. 2021; Latif et al. 2021; Tehrani et al. 2022). Rafiei and Adeli (2017) propose a novel earthquake early warning model based on neural dynamic classification and optimization. In the present study, FNN provided
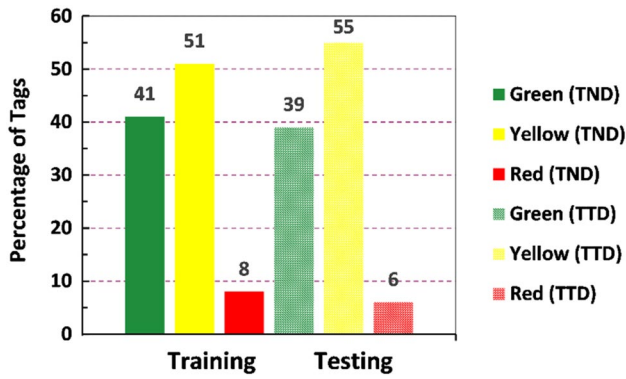
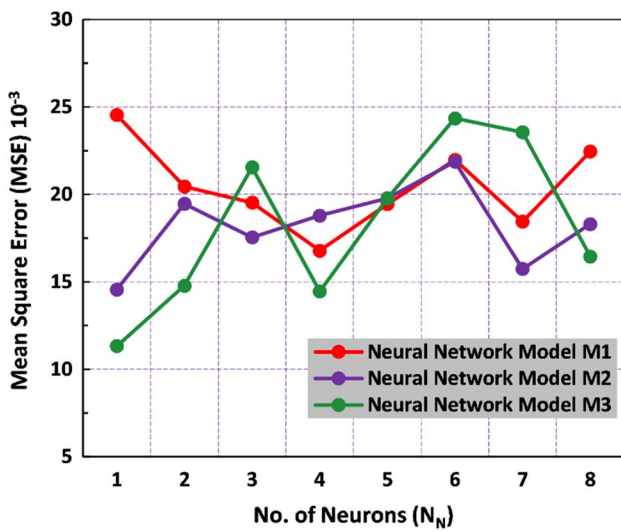**Fig. 6** Tag distribution of various classes for training and testing data sets

Fig. 7 Filtration of error and selection of best neural network model in the present study

the cumulative weightage factor for the output layer. At the initial stage, the weightage factor of all input–output data sets is combined to make the relationship between the specified input variable through training the neurons. After

the neurons have been trained, target data are utilized to test the robustness of the network line.

The tag scattering for the training and testing data sets is depicted in Fig. 6. For class RED, tagging percentages of around 8 and 6 were recorded for data picked for training and testing, respectively. The influence of these data sets is evaluated for three neuron apportionment scenarios. As illustrated in Fig. 7, neural network Model 2 produced an average level of Mean Square Error (MSE) and is used as the desired network for further predictive modelling.

Table 6 displays the results of both the training and testing data sets. Both data sets have demonstrated great performance in terms of specified criteria.

The weightage factors are finalized through conceivable hits and trials, and a mathematical equation in terms of damage index is established. This provides the possible damage states for post-seismic scenarios. Neural networks aided in the identification of damage by robotizing the procedure and obtaining sustainable perfection pitch. The generalized form of the mathematical equation presenting the prediction model is presented in Eq. 1.

$$\ln(DI) = A + B \tag{1}$$

where, $A = \left[\dfrac{(SSD \times OD^{0.002}) + \left(\frac{PGA}{t} \right)^{4.2}}{GSI + \Phi^{4.2}} \right]$ and $B = 1.15$. The factor "A" is the damage governing factor. The range values of A for different damage states are urged in Table 7.

The final form of the Seismic Tunnel Damage Prediction (STDP) Model is given in Eq. 2.

$$\ln(DI) = \left[\dfrac{(SSD \times OD^{0.002}) + \left(\frac{PGA}{t} \right)^{4.2}}{GSI + \Phi^{4.2}} \right] + 1.15 \tag{2}$$

Seismic hazard analysis can be utilized to get the seismic input variables (PGA and SSD) used in Eq. 2. Aside from these two, the rest of the criteria can be found in the planning and execution reports of any infrastructure project. Equation 2 can be solved for any damage state if the required variables are available. The seismic demand and capacity

Table 6 Attributes of STDP model during training and testing phase

Attributes	Mathematical relationship	Training	Testing
Accuracy	$\frac{TP+TN}{P+N}$	1	0.97
Sensitivity	$\frac{TP}{P}$	1	0.95
Specificity	$\frac{TN}{N}$	1	0.99
Φ correlation coefficient	$\frac{TP.TN-FP.FN}{\sqrt{(TP+FN).(TN+FP).(TP+FP).(TN+FN)}}$	1	0.97
Precision, Recall F measure	$\frac{1}{\gamma(1/P)+\frac{1-\gamma}{R}}$	1.00, 0.84	0.98, 0.83

TP True positive, *FP* False positive, *TN* True negative, *FN* False negative, *P* Positive sample, *N* Negative sample, γ Mean balance (0.5), *R* Recall

Table 7 Proposed ranges of Damage Index (DI) for various damage states(*DS*)

Seismic tunnel damage		Proposed range of damage index (DI)	Average damage index (DI$_{avg}$)
Damage states	Notations		
None (DS_0)	DS_0	< 2.5	–
Minor (DS_1)	DS_{1A}	2.6-3.0	2.8
	DS_{1B}	3.1–3.5	3.3
Moderate (DS_2)	DS_{2A}	3.6-4.0	3.75
	DS_{2B}	4.1–4.5	4.3
Extensive (DS_3)	DS_{3A}	4.6-5.0	4.8
	DS_{3B}	5.1-5.5	5.3
	DS_{3C}	5.6-6.0	5.8
Collapse (DS_4)	DS_{4A}	6.1-7.0	6.5
	DS_{4B}	> 7.0	-

can be estimated backward based on the proposed damage states. This computation will be useful for any design revisions in seismically-prone tunnelling projects.

Results

Performance assessment of proposed prediction model

The proposed mathematical equation-based prediction model can be used to evaluate the damage scenarios for underground structures located in seismic-prone areas. In the discipline of predictive modelling, performance evaluation is a critical step after developing a model or equation. The R Score is used to assess the proposed model presented in Eq. 2. *R* values vary from 0 to 1 and can be calculated using Eq. 3.

$$R = \frac{TP}{TP + FN} - \frac{FP}{TN + FP} \qquad (3)$$

In this study, G125-25-25 was identified as one of the best data sets, with *R* value of 0.2157. Table 8 displays performance indicators for all defined data sets. RG25-25-25 is the best arbitrary data set that was identified through random sequencing. Table 9 highlights a list of arbitrary data sets and their performances.

Validation of proposed prediction model

The Seismic Tunnel Damage Prediction (STDP) Model proposed in the present study is compared with the tunnel damage data sets from the 1999 Chi-Chi earthquake, the 2004 Mid-Niigata earthquake, and the 2008 Wenchuan earthquake. Table 10 summarizes the damage states of

Table 8 Performance assessment of selected data set for proposed STDP Model

Group	TP	FN	FP	TN	R score
G25-25-25	2	21	4	87	0.0430
G50-25-25	7	18	11	54	0.1108
G75-25-25	17	21	32	46	0.0371
G100-25-25	45	67	35	66	0.0553
G125-25-25	43	25	45	63	0.2157
G150-25-25	59	45	64	51	0.0108
G175-25-25	54	43	33	57	0.1900
G200-25-25	4	27	9	75	0.0219

Table 9 Performance assessment of arbitrary data set for proposed STDP Model

Group	TP	FN	FP	TN	R score
RG25-25-25	12	32	2	19	0.1775
RG50-25-25	54	32	59	56	0.1149
RG75-25-25	18	22	34	44	0.0141
RG100-25-25	19	15	12	14	0.0973
RG125-25-25	10	15	32	63	0.0632
RG150-25-25	64	25	54	25	0.0356
RG175-25-25	9	7	18	16	0.0331
RG200-25-25	8	7	73	75	0.0401

Table 10 Percentage of damaged tunnels during historical earthquake events

Damage states	Notations	1999 Chi-Chi earthquake	2004 Mid-Niigata earthquake	2008 Wenchuan earthquake
None (DS_0)	DS_0	6	23	10
Minor (DS_1)	DS_{1A}	4	12	8
	DS_{1B}	3	2	15
Moderate (DS_2)	DS_{2A}	11	2	18
	DS_{2B}	17	19	9
Extensive (DS_3)	DS_{3A}	7	5	3
	DS_{3B}	23	11	8
	DS_{3C}	29	24	25
Collapse (DS_4)	DS_{4A}	0	1	2
	DS_{4B}	0	1	2

tunnels affected by these three seismic events. The correlation coefficient (R), mean absolute error (MAE), mean absolute percent error (MAPE), and root mean squared error (RMSE) are considered as system governing markers (SGM) to execute the proposed STDP model. These markers are estimated using the following mathematical relationships (Eqs. 4 to 7).

Table 11 PGA based execution of STDP Model with other DL models for historically damaged tunnels

Marker	STDP Model (Present Study)	1999 Chi-Chi Earthquake (CETD Model)	2004 Mid-Niigata Earthquake (NETD Model)	2008 Wenchuan Earthquake (WETD Model)
R	0.914	0.871	0.925	0.893
MAE	0.257	0.189	0.253	0.249
MAPE	0.203	0.192	0.215	0.255
RMSE	0.387	0.452	0.394	0.496

$$R = \frac{\sum(x_i - \bar{x})(y_i - \bar{y})}{\sqrt{\sum(x_i - \bar{x})^2 \sum(y_i - \bar{y})^2}} \tag{4}$$

$$MAE = \frac{\sum_{i=1}^{N}\left(|x_i - y_i|\right)}{N} \tag{5}$$

$$MAPE = \frac{\sum_{i=1}^{N}\left(\frac{x_i - y_i}{x_i}\right)}{N} \tag{6}$$

$$RMSE = \sqrt{\frac{\sum(x_i - y_i)^2}{N}} \tag{7}$$

N, x_i, y_i, $\bar{x}$ and $\bar{y}$ are the total number of data sets, measured output, estimated output, mean measured value, and mean estimated value, respectively. SGM considers PGA as a major input variable, for the proposed model and actual models of the previous earthquake are enlisted in Table 11. The suggested model can accurately estimate *DI* because the data points are typically placed close to the perfect fit, where predictions match observations. For the 2004 Mid-Niigata earthquake, the R-value for the suggested STDP model and the NETD model is nearly comparable. The MAE for the CETD Model differs from others since the data set for the Chi-Chi earthquake was found to be unevenly distributed. However, the proposed model is determined to be the best fit with the NETD and WETD models. The proposed model's good performance for the Himalayan region with acceptable predictive ability and accurate performance on testing data demonstrates the model's potential to predict the damage states for earthquakes in diverse ground scenarios covered by structural heterogeneity.

Considering the percentile effect of all input variables, an analogous study of all prediction models is done. The comparison of the proposed damage index ($DI_{proposed}$) and actual damage index (DI) are presented in Fig. 8. The STDP model has a somewhat considerable variance from the other models. The data from the CETD model
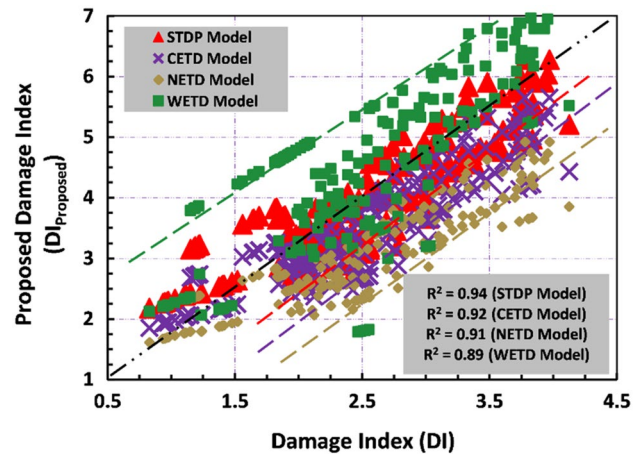
Fig. 8 Comparison between the proposed STDP model with other models for historical earthquakes

Table 12 Revised values for input variables

Input variables	Minimum	Maximum
Source to site distance (SSD), km	0.01	500.0
Peak Ground Acceleration (PGA), g	0.1	1.0
Overburden Depth (OD), km	5.0	500.0
Lining Thickness (t), mm	250	1000
Tunnel Diameter (Φ), m	3.0	10.0
Geological Strength Index (GSI)	0.0	100.0

are closer to the 1:1 line, indicating a stronger connection between the measured and anticipated data values. When comparing the proposed model to the WETD model, the DL neural network computes a higher value of *R*. As a result, the DL-based prediction model can be used securely to calculate the DI for the seismic design of the tunnels under consideration during post-seismic scenarios.

It should be clear that the range of the training data limits the validity of the DL-based prediction model. For the best fitting of all models, the ranges of input variables are revised to develop the seismic design guidelines for tunnelling (Table 12).
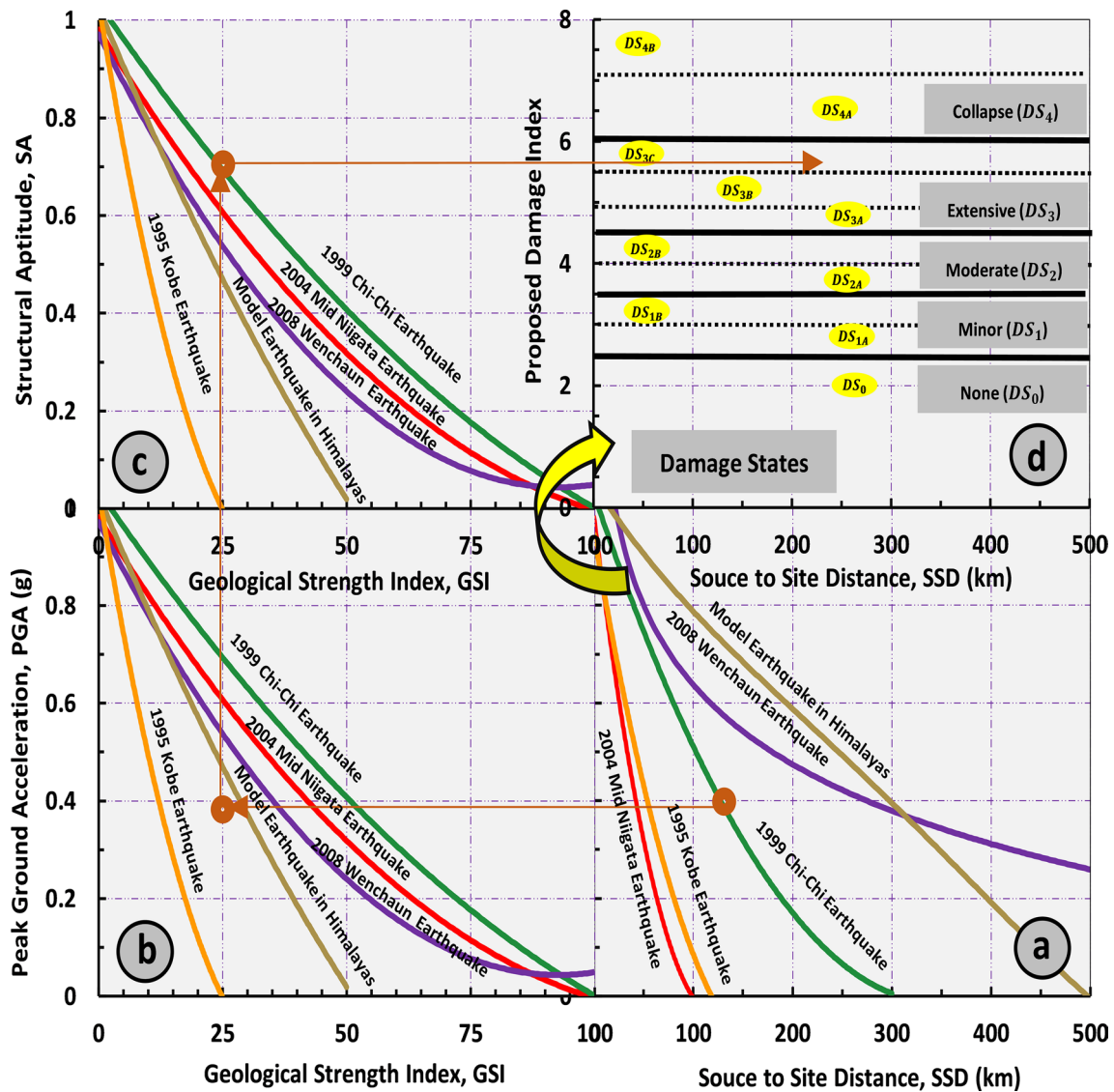
Fig. 9 Seismic tunnel damages (STD) multi-graph for damage states prediction

Discussions

The seismic vulnerability depicts the probability of a region or any structural constituent of infrastructure projects being damaged during a ground motion with the maximum peak ground acceleration for a defined set of epicentral distance and earthquake magnitude of a specific event. The risk reduction process involves both active and passive steps. Active steps involve avoiding or reducing hazards, while passive steps involve choosing particular mitigation methods (Kim et al. 2020). Seismic design guidelines are required to obtain a clear picture of the expected damages and level of vulnerability to which the structure is subjected. The data set of the Himalayan region, with a focus on the USBRL project and previous devastating

earthquakes that triggered underground utilities, such as the 1995 Kobe earthquake, the 1999 Chi-Chi earthquake, the 2004 Mid-Niigata earthquake, and the 2008 Wenchuan earthquake, were considered to back-calculate the damage governing parameters using proposed Seismic Tunnel Damage Prediction (STDP) model. The seismic design guidelines provided considering historical case studies by fitting all data in the proposed model. For this purpose, input variables are accounted within the revised limit as suggested in Table 12. The "STD multiple graphs" shown in Fig. 9, is a four-sector graph based on the logical order of the input variables. The comparison of peak ground acceleration (PGA) and source-to-site distance (SSD) from an earthquake deaggregation data set is shown in Graph I (bottom right quadrant). Based on the deaggregation setup

Table 13 Seismic design guidelines for damage states and mitigation recommendations for tunnelling projects

Seismic tunnel damage states		Pattern of damages		Crack specifications			Proposed range of damage index (DI)
		Portal	Lining	Types	Width (mm)	Length (m)	
None (DS_0)		–	–	–	–	–	<2.5
Minor (DS_1)	(DS_{1A})	Small rock falls	Minor cracking	Shear	<2	<3	2.6–3.0
	(DS_{1B})	Invert heave	Minor spalling	Ring	2–5	4–5	3.1–3.5
Moderate (DS_2)	(DS_{2A})	Small rock topple and sliding	Small cracking	Oblique	6–15	6–8	3.6–4.0
	(DS_{2B})	Crown settlement	Small spalling	Cracking of shotcrete	16–30	9–10	4.1–4.5
Extensive (DS_3)	(DS_{3A})	Large slumps of soil or rock mass	Large cracking and Spalling	Cracking of arch	31–50	11–15	4.6–5.0
	(DS_{3B})	Deep sliding	Large falling	Cracking of side walls	51–75	16–20	5.1–5.5
	(DS_{3C})	Crown settlement and deep sliding	Exfoliation of concrete lining	Longitudinal	76–85	21–25	5.6–6.0
Collapse (DS_4)	(DS_{4A})	Possible chances of landslides	Complete collapse	Longitudinal and ring	85–100	26–35	6.1–7.0
	(DS_{4B})	Complete collapse	Exfoliation of concrete lining and large racking and spalling	Cracking of shotcrete; shear zones	>100	>35	>7.0

Seismic tunnel damage states		Risks		Serviceability	Mitigation measures
		Safety Risk	Operational Risk		
None (DS_0)		–	Normal operation	Accessible	
Minor (DS_1)	(DS_{1A})	Possible fall of debris	Possible disruption of traffic; collapse of the frontal slope		Pretensioned rock bolts or steel struts with steel fiber reinforced shotcrete (SFRS) can be used to give support. Debris flow barriers, multiple check dams, diversion berms, catchment basins, material flow racks, or breakers can be valued to forfend debris from falling.
	(DS_{1B})	Possibility of water leakage			Water leakage is primarily caused by ground water flowing parallel to the slope; this level should be performed as far away from the slope face as possible to avoid failure, and this can be accomplished by installing perforated drain pipes wrapped in a geotextile type 3 membrane. To address leakage difficulties, pressurized grouting might be used.
Moderate (DS_2)	(DS_{2A})	Fall of debris; water seepage through construction joints	Disruption of traffic; collapse of frontal slope	Accessible with moderate repair	Grouting or employing a whole column grouted rock to anchor to support the ground.
	(DS_{2B})	Water leakage	Cracking of shotcrete		The liner can be sealed with either chemical or cementitious grout. Amine and polyester resins are jabbed into concrete cracks.

Table 13 (continued)

Seismic tunnel damage states		Risks		Serviceability	Mitigation measures
		Safety Risk	Operational Risk		
Extensive (DS_3)	(DS_{3A})	Fall of debris; seepage through the side wall	Disruption of traffic with delay in travel time	Inaccessible	Grouting of rock mass fissures can be done.
	(DS_{3B})	Water leakage from juncture; distortion of steel supports	Side wall deformation		Determine the source of the leak and divert or grout the ground outside the tunnel to form a "blister" fix that shuts off the leak.
	(DS_{3C})	Water ingress problems; compressive buckling in bed	Delay in travel time; Uplifting of side wall		
Collapse (DS_4)	(DS_{4A})	Slope instability issues; deformation in sidewall	Congestion of drainage ditches		Spalls in tunnels are repaired using the form-and-pour method of concrete installation or by hand application of cementitious mortars including polymers. Amine and polyester resins are injected into cracks in concrete.
	(DS_{4B})	Landslide susceptibility	Damage of wire rope protection nets		

provided in Graph I, Graph II (bottom left quadrant) determines the geological strength index (GSI). Graph III (top left quadrant) calculates structural aptitude (SA) from geological strength index (GSI) and earthquake deaggregation setup. SA can be estimated using the following Eq. 8.

$$SA = \frac{0.3 \times t \times OD}{\Phi^2} \tag{8}$$

The probable damage states are predicted using structural aptitude (SA) and geological strength index (GSI), which are reobserved after deaggregation, as shown in Graph IV (top right quadrant). The seismic tunnel damages can be categorized into five major groups. They are none (DS_0), minor (DS_1), moderate (DS_2), extensive (DS_3), and collapse (DS_4). The subgrouping is also given for scenarios where the damage index (DI) is more than 2.5. The damage states produced in Fig. 9 are utilized as a starting point to prepare the seismic design guidelines shown in Table 13. These design guidelines detail damage indexing, damage pattern, and crack predictive specification. It also discusses the risks involved and their consequences on transportation network serviceability. Mitigation steps that must be implemented are also recommended for all projected damage states.

Conclusion

Soft computing advancements have influenced researchers from various fields to adopt the technology and move forward with artificial intelligence. Based on the purpose and availability of prerequisites, the neural network is trained in the deep learning (DL) technique. A few essential research problems cannot be tackled using traditional methods. In such instances, the concept of the deep learning-based

mathematical solution is a boon. Understanding the effects of earthquakes on structures necessitates prior experience with historical data sets. This requires the selection of input variables as well as the prior estimation of predicted outcomes. Using data from the Himalayan region, this study attempted to develop a mathematical formulation-based Seismic Tunnel Damage Prediction (STDP) model. To define the neural network's input layers, site-specific data baskets with peak ground acceleration (PGA), source to site distance (SSD), overburden depth (OD), lining thickness (t), tunnel diameter (Φ), and geological strength index (GSI) are used. 70% of the data set from the Himalayan region is used to train the Feedforward Neural Network (FNN). The remaining 30% of the data is used to test the model after training. The weightage factors are determined through conceivable hits and trials, and a mathematical equation in terms of damage index is established. This model predicts the potential damage states for tunnels under various post-seismic scenarios.

The validation of the STDP model with other models based on historical earthquakes demonstrated its efficiently processing nature for minor instinctive shrewdness. Seismic demand and capacity can be estimated backward based on the proposed damage states. With an R-value of 0.2157, G125-25-25 was identified as one of the best data sets. The proposed model best fits the NETD (2004 Mid-Niigata Earthquake) and WETD (2008 Wenchuan Earthquake) models. After accounting for damaged tunnel data from the 1995 Kobe earthquake, 1999 Chi-Chi earthquake, 2004 Mid-Niigata earthquake, and 2008 Wenchuan earthquake, input variables are modified to fit all in a way that follows a common trend line. The "STD multiple graphs" are also provided, which aid in identifying potential damage states in future earthquakes. The seismic design guidelines

include mitigation methods for all probable damage states. The proposed Seismic Tunnel Damage Prediction (STDP) model, STD multiple graphs, and design guidelines can be used for any earthquake-prone tunnelling project anywhere in the world.

Declarations

Conflict of interest The authors have no relevant financial or non-financial interests to disclose.

References

Abdulnaby W, Al-Mohmed R, Mahdi M (2016) Seismicity and recent stress regime of Diyala City, Iraq–Iran border. Model Earth Syst Environ 2(3):1–8

Ahmad A, Dhang PC (2019) Methodologies for the geological and geotechnical works during the construction of railway tunnels in Himalayan region, India. Him Prabhat XII:28–36

Alhassan DU, Obiora DN, Okeke FN, Ibuot JU (2018) Investigation of groundwater potential of southern Paiko, northcentral Nigeria, using seismic refraction method. Model Earth Syst Environ 4(2):555–564

Ansari A, Zahoor F, Rao KS, Jain AK (2022b) Liquefaction hazard assessment in a seismically active region of Himalayas using geotechnical and geophysical investigations: A case study of Jammu region, Jammu and Kashmir. Bull Eng Geol Environ 81(349):1–19. https://doi.org/10.1007/s10064-022-02852-3

Ansari A, Zahoor F, Rao KS, Jain AK (2022a) Seismic hazard assessment studies based on deterministic and probabilistic approaches for the Jammu region, NW Himalayas. Arab J Geosci 15(11):1–26. https://doi.org/10.1007/s12517-022-10330-z

Asakura T, Sato Y (1996) Damage to mountain tunnels in hazard area. Soils Found 36:301–310

Aydan Ö, Ohta Y, Geniş M, Tokashiki N, Ohkubo K (2010) Response and stability of underground structures in rock mass during earthquakes. Rock Mech Rock Eng 43(6):857–875

Barrow H (1996) Connectionism and neural networks. Artificial intelligence. Academic Press, pp 135–155

Bernardi MS, Africa PC, De Falco C, Formaggia L, Menafoglio A, Vantini S (2021) On the Use of Interferometric Synthetic Aperture Radar Data for Monitoring and Forecasting Natural Hazards. Math Geosci 53(8):1781–1812

Biswas S, Sinha M (2021) Performances of deep learning models for Indian Ocean wind speed prediction. Model Earth Syst Environ 7(2):809–831

Biswas RN, Islam M, Islam MN (2018) Modeling on management strategies for spatial assessment of earthquake disaster vulnerability in Bangladesh. Model Earth Syst Environ 4(4):1377–1401

Callisto L, Ricci C (2019) Interpretation and back-analysis of the damage observed in a deep tunnel after the 2016 Norcia earthquake in Italy. Tunn Undergr Space Tech 89:238–248

Chen H, He X, Teng Q, Sheriff RE, Feng J, Xiong S (2020) Super-resolution of real-world rock microcomputed tomography images using cycle-consistent generative adversarial networks. Phys Rev E 101(2):023305

Dalguer LA, Irikura K, Riera JD (2003) Generation of new cracks accompanied by the dynamic shear rupture propagation of the 2000 Tottori (Japan) earthquake. Bull Seismol Soc Am 93(5):2236–2252

Dang HV, Raza M, Nguyen TV, Bui-Tien T, Nguyen HX (2021) Deep learning-based detection of structural damage using time-series data. Struct Infrastruct Eng 17(11):1474–1493

Derakhshani A, Foruzan AH (2019) Predicting the principal strong ground motion parameters: A deep learning approach. Appl Soft Comput 80:192–201

Dickey J, Borghetti B, Junek W (2019) Improving regional and teleseismic detection for single-trace waveforms using a deep temporal convolutional neural network trained with an array-beam catalog. Sensors 19(3):597

Dimililer K, Dindar H, Al-Turjman F (2021) Deep learning, machine learning and internet of things in geophysical engineering applications: An overview. Microprocess Microsyst 80:103613

Durrani AJ, Elnashai AS, Hashash Y, Kim SJ, Masud A (2005) The Kashmir earthquake of October 8, 2005: A quick look report. MAE Center CD Release 05 – 04

Falcone R, Lima C, Martinelli E (2020) Soft computing techniques in structural and earthquake engineering: a literature review. Eng Struct 207:110269

Foucquier A, Robert S, Suard F, Stéphan L, Jay A (2013) State of the art in building modelling and energy performances prediction: A review. Renew Sustain Energy Rev 23:272–288

Fukushima K, Miyake S (1982) Neocognitron: A new algorithm for pattern recognition tolerant of deformations and shifts in position. Pattern Recogn 15(6):455–469

Harichandran RS, Vanmarcke EH (1986) Stochastic variation of earthquake ground motion in space and time. J Eng Mech 112(2):154–174

Hashash YMA, Hook JJ, Schmidt B, John I, Yao C (2001) Seismic design and analysis of underground structures. Tunn Undergr Space Technol 16(4):247–293

Hinton G, Salakhutdinov R (2012) An efficient learning procedure for deep Boltzmann machines. Neural Comput 24(8):1967–2006

Hoang ND, Tran VD (2019) Image processing-based detection of pipe corrosion using texture analysis and metaheuristic-optimized machine learning approach. Computational intelligence and neuroscience

Huang JP, Wang XA, Zhao Y, Xin C, Xiang H (2018) Large earthquake magnitude prediction in Taiwan based on deep learning neural network. Neural Netw World 28(2):149–160

Huang Z, Argyroudis SA, Pitilakis K, Zhang D, Tsinidis G (2022) Fragility assessment of tunnels in soft soils using artificial neural networks. Undergr Space 7(2):242–253

Ihueze CC, Onwurah UO (2018) Road traffic accidents prediction modelling: An analysis of Anambra State, Nigeria. Accid Anal Prev 112:21–29

Jiang Y, Wang C, Zhao X (2010) Damage assessment of tunnels caused by the 2004 Mid Niigata Prefecture Earthquake using Hayashi's quantification theory type II. Nat Hazards 53(3):425–441

Jordan MI, Mitchell TM (2015) Machine learning: Trends, perspectives, and prospects. Science 349(6245):255–260

Kalakonas P, Silva V (2022) Seismic vulnerability modelling of building portfolios using artificial neural networks. Earthq Eng Struct Dynamics 51(2):310–327

Kim T, Song J, Kwon OS (2020) Probabilistic evaluation of seismic responses using deep learning method. Struct Saf 84:101913

Kochhar A, Singh H, Sahoo S, Litoria PK, Pateriya B (2022) Prediction and forecast of pre-monsoon and post-monsoon groundwater level: using deep learning and statistical modelling. Model Earth Syst Environ 8(2):2317–2329

Konagai K, Numada M, Zafeirakos A, Johansson J, Sadr A, Katagiri T (2005) An example of landslide-inflicted damage to tunnel in the 2004 Mid-Niigata Prefecture earthquake. Landslides 2(2):159–163

Kong Q, Trugman DT, Ross ZE, Bianco MJ, Meade BJ, Gerstoft P (2019) Machine learning in seismology: Turning data into insights. Seismol Res Lett 90(1):3–14

Kontoe S, Zdravkovic L, Potts DM, Menkiti CO (2008) Case study on seismic tunnel response. Can Geotech J 45(12):1743–1764

Kumar P (2018) Slip forming: sharing an experience at bridge no. 43, Bakkal of USBRL project. Him Prabhat X:72–81

Lai J, He S, Qiu J, Chen J, Wang L, Wang K, Wang J (2017) Characteristics of seismic disasters and aseismic measures of tunnels in Wenchuan earthquake. Environ Earth Sci 76(2):1–19

Latif SD, Ahmed AN, Sathiamurthy E, Huang YF, El-Shafie A (2021) Evaluation of deep learning algorithm for inflow forecasting: a case study of Durian Tunggal Reservoir, Peninsular Malaysia. Nat Hazards 109(1):351–369

Mangalathu S, Burton HV (2019) Deep learning-based classification of earthquake-impacted buildings using textual damage descriptions. Int J Disaster Risk Reduct 36:101111

Meraj G, Farooq M, Singh SK, Islam M, Kanga S (2021) Modeling the sediment retention and ecosystem provisioning services in the Kashmir valley, India, Western Himalayas. Model Earth Syst Environ. https://doi.org/10.1007/s40808-021-01333-y

Mosavi A, Ozturk P, Chau KW (2018) Flood prediction using machine learning models: Literature review. Water 10(11):1536

Nahata D, Mulchandani HK, Bansal S, Muthukumar G (2019) Post-earthquake assessment of buildings using deep learning. arXiv preprint arXiv:1907.07877

Nanda AM, Yousuf M, Tali PA, Ul Hussan Z, Ahmed P (2021) Assessment of earthquake-triggered landslides along NH 1D in J&K, India: using multivariate approaches. Model Earth Syst Environ. https://doi.org/10.1007/s40808-021-01322-1

Ohmachi T (2000) On damage to dams in Taiwan due to the 1999 Chichi earthquake. J Jpn Soc Dam Eng 10(2):138–150

Ornthammarath T, Corigliano M, Lai CG (2008) Artificial neural networks applied to the seismic design of deep tunnels. In 14th World Conference in Earthquake Engineering

Özdamar L, Pedamallu CS (2011) A comparison of two mathematical models for earthquake relief logistics. Int J Logistics Syst Manag 10(3):361–373

Pascanu R, Mikolov T, Bengio Y (2013) On the difficulty of training recurrent neural networks. In International conference on machine learning. PMLR. pp. 1310–1318

Patterson B, Leone G, Pantoja M, Behrouzi AA (2018) Deep learning for automated image classification of seismic damage to built infrastructure. In Eleventh US National Conference on Earthquake Engineering

Phoon KK (2020) The story of statistics in geotechnical engineering. Georisk Assess Manage Risk Eng Syst Geohazards 14(1):3–25

Raaj S, Pathan AI, Mohseni U, Agnihotri PG, Patidar N, Islam M, Patidar S (2022) Dam site suitability analysis using geo-spatial technique and AHP: a case of flood mitigation measures at Lower Tapi Basin. Model Earth Syst Environ. https://doi.org/10.1007/s40808-022-01441-3

Rafiei MH, Adeli H (2017) NEEWS: a novel earthquake early warning model using neural dynamic classification and neural dynamic optimization. Soil Dyn Earthq Eng 100:417–427

Rajesh K, Agarwal R (2013) Sangaldan station in tunnel. Him Prabhat18–20

Ram P (2015) Tunnelling through water bearing strata. Him Prabhat44–51

Riella A, Quaglio G, Sikka V, Zammit H (2019) Tackling squeezing ground during tunnel T1 excavation. Him Prabhat XII:16–27

Rohilla V, Surinder P (2018) Tunnel lighting in railway tunnel projects & dialux simulation for tunnel T-49 (Udhampur-Srinagar-Baramulla new BG railway line project). Him Prabhat X:32–37

Roy N, Sarkar R (2017) A review of seismic damage of mountain tunnels and probable failure mechanisms. Geotech Geol Eng 35(1):1–28

Sharma A, Panwar AM (2017) Rock fall protection solutions on tunnel portals. Him Prabhat VIII:42–46

Sharma HK, Manchanda H (2018) Instrumentation and monitoring of tunnel T2 (between km. 33 + 212 to km. 38 + 375 of Katra to Dharam section of Udhampur Srinagar Baramula new BG railway project. Him Prabhat X:14–31

Shrestha R, Li X, Yi L, Mandal AK (2020) Seismic damage and possible influencing factors of the damages in the Melamchi tunnel in Nepal due to Gorkha earthquake 2015. Geotech Geol Eng 38(5):5295–5308

Singh J, Sherpuri A (2018) Geology of the Anji Bridge alignment on Katra- Qazikund rail line section, USBRL project, Reasi district (Jammu & Kashmir). Him Prabhat X:65–68

Talkhablou M, Kianpour M, Fatemi Aghda SM (2019) ArcGIS fuzzy modeling to assess the relationship between seismic wave velocity and electrical resistivity with limestone mass quality (case study: Asmari Formation, southwest Iran). Model Earth Syst Environ 5(3):1025–1035

Tehrani FS, Calvello M, Liu Z, Zhang L, Lacasse, (2022) Machine learning and landslide studies: recent advances and applications. Nat Hazards. https://doi.org/10.1007/s11069-022-05423-7

Tomar BBS, Kumar A (2013) Implications of Himalayan geology in TBM working. Him Prabhat60–64

Tsinidis G, de Silva F, Anastasopoulos I, Bilotta E, Bobet A, Hashash YMA, He C, Kampas G, Knappett G, Madabhushi G, Nikitas N, Pitilakis K, Silvestri F, Viggiani R, Fuentes R (2020) Seismic behaviour of tunnels: from experiments to analysis. Tunn Undergr Space Tech 99:103334

Valaskova K, Kliestik T, Svabova L, Adamko P (2018) Financial risk measurement and prediction modelling for sustainable development of business entities using regression analysis. Sustainability 10(7):2144

Wang ZZ, Zhang Z (2013) Seismic damage classification and risk assessment of mountain tunnels with a validation for the 2008 Wenchuan earthquake. Soil Dyn Earthq Eng 45:45–55

Wang TT, Kwok OLA, Jeng FS (2021) Seismic response of tunnels revealed in two decades following the 1999 Chi-Chi earthquake (Mw 7.6) in Taiwan. Rev Eng Geol 287:106090

Wani AR, Alamgir J (2017) Case study of tunnel T40-41 in Sangaldan area of USBRL project. Him Prabhat IX:11–23

Wingler FA (2020) The Gap in the missing Link Katra - Banihal.Him Prabhat1–36

Xia C, Pan Z, Polden J, Li H, Xu Y, Chen S (2022) Modelling and prediction of surface roughness in wire arc additive manufacturing using machine learning. J Intell Manuf 33(5):1467–1482

Xu Y, Wei S, Bao Y, Li H (2019) Automatic seismic damage identification of reinforced concrete columns from images by a region-based deep convolutional neural network. Struct Control Health Monit 26(3):e2313

Xue Y, Li Y (2018) A fast detection method via region-based fully convolutional neural networks for shield tunnel lining defects. Comput Aided Civil Infrastruct Eng 33(8):638–654

Yu HT, Chen JT, Yuan Y, Zhao X (2016) Seismic damage of mountain tunnels during the 5.12 Wenchuan earthquake. J Mt Sci 13(11):1958–1972

Yuan X, Li L, Wang Y (2019) Nonlinear dynamic soft sensor modeling with supervised long short-term memory network. IEEE Trans Industr Inf 16(5):3168–3176

Yusoff R, Adhikari KN (2017) Geological studies for construction of T-74R- problems and solutions. Him Prabhat VIII:28–47

Zhang L, Pan Y (2022) Information fusion for automated post-disaster building damage evaluation using deep neural network. Sustain Cities Soc 77:103574

Zhang X, Jiang Y, Sugimoto S (2018) Seismic damage assessment of mountain tunnel: a case study on the Tawarayama tunnel due to the 2016 Kumamoto Earthquake. Tunn Undergr Space Tech 71:138–148

Zhang W, Li H, Li Y, Liu H, Chen Y, Ding X (2021) Application of deep learning algorithms in geotechnical engineering: a short critical review. Artif Intell Rev 54(8):5633–5673

Zhang P, Yin ZY, Jin YF (2022) Bayesian neural network-based uncertainty modelling: application to soil compressibility and undrained shear strength prediction. Can Geotech J 59(4):546–557

Zhao X, Coates G, Xu W (2019) A hierarchical mathematical model of the earthquake shelter location-allocation problem solved using an interleaved MPSO–GA. Geomatics Nat Hazards Risk 10(1):1712–1737

Zhu L, Peng Z, McClellan J, Li C, Yao D, Li Z, Fang L (2019) Deep learning for seismic phase detection and picking in the aftershock zone of 2008 Mw7. 9 Wenchuan Earthquake. Phys Earth Planet Inter 293:106261